New journal of chemistry

Supporting Information

Rapid iodine adsorption from vapor phase and solution by a nitrogen-rich covalent piperazine-triazine-based polymer

Yalin Huang[a,#], Wei Li[b,#], Yuwei Xu[a], Mu Ding[a], Jie Ding[a], Yun Zhang[a], Yuanhua Wang[a], Shanyong Chen[a], Yongdong Jin*[,a], Chuanqin Xia*[,a]

[a] College of Chemistry, Sichuan University, Chengdu 610064, China.

[b] Department of Cardiothoracic Surgery, Chengdu 610500, China.

[#] These authors contributed equally to this work.

*Corresponding authors:

Prof. Y. Jin and Prof. C. Xia

College of Chemistry, Sichuan University

Chengdu, 610064, China

Tel.: +86-28-85412343 (Y. Jin and C. Xia).

E-mail: jinyongdong@scu.edu.cn (Y. Jin), xiachqin@163.com (C. Xia).

I. General procedures for iodine uptake

Section. 1 Iodine adsorption in solution

The iodine adsorption experiments in solution were carried out in the following.[1, 2] 10 mg of n-CTP and 20 mL cyclohexane solutions of iodine were added to a sealed Erlenmeyer flask to form a mixture solution that was stirred at room temperature. The solid was isolated by centrifugation (8000 rpm, 3 min), and the concentrations of iodine remained in cyclohexane solution were analyzed by UV/vis spectra using the working curve established (Figure S7). The adsorption capacity (q_e, mg g^{-1}) was calculated by the Eq. S1, and the iodine removal efficiency (R, %) was calculated using the Eq. S2. All tests were carried out at least three times.

$$q_e = \frac{(c_0 - c_e)V}{m} \quad \text{(S1)}$$

$$R = \left(1 - \frac{c_e}{c_0}\right) \times 100\% \quad \text{(S2)}$$

where c_0, c_e is concentrations of iodine in cyclohexane solution before and after the adsorption of iodine, respectively.

Section. 2 Kinetic models of the iodine adsorption by n-CTP.

The adsorption data were fitted by the pseudo-first order (Eq. S3) and pseudo-second order (Eq. S4) models to evaluate the controlling mechanism of the iodine adsorption process. The linear forms of the two models can be expressed as follows:

$$\ln(q_e - q_t) = \ln q_e - k_1 t \quad \text{(S3)}$$

$$\frac{t}{q_t} = \frac{1}{k_2 {q_e}^2} + \frac{1}{q_e} t \quad \text{(S4)}$$

where q_e and q_t (g g^{-1}) are the adsorption capacity of iodine at saturated time and time t (min), respectively. k_1 (min^{-1}) and k_2 (g g^{-1} min^{-1}) represents the rate constant of the pseudo-first-order model and pseudo-second-order model respectively.

Section. 3 Isotherm models of iodine adsorption by n-CTP

To understand the adsorption mechanism, the Langmuir and Freundlich models were used to simulate the adsorption profiles. Langmuir model represents monolayer sorption based on the hypothesis that all the sorption sites have equal affinity and that desorption at one site doesn't influence an adjacent site, which can be described as Eq. S5:

$$\frac{1}{q_e} = \frac{1}{q_m} + \frac{1}{K_L q_m} \frac{1}{C_e} \quad \text{(S5)}$$

where K_L (L mg^{-1}) is the Langmuir constant, which is related to the affinity of binding sites, and q_m (mg g^{-1}) is the maximum adsorption capacity.

The Freundlich model can be applied for multilayer sorption and the sorption on heterogeneous surfaces, which can be described as Eq. S6:

$$\ln q_e = \ln K_F + \frac{1}{n} \ln C_e \quad \text{(S6)}$$

where K_F and n are the Freundlich constants related to sorption capacity and sorption intensity, respectively.

II. Characterization of n-CTP

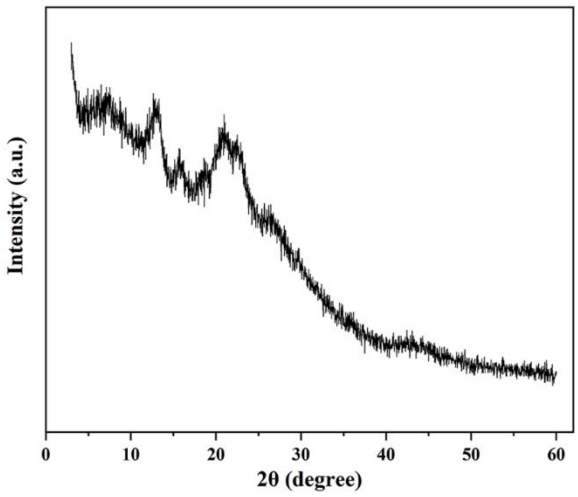

Fig. S1 PXRD patterns of n-CTP.

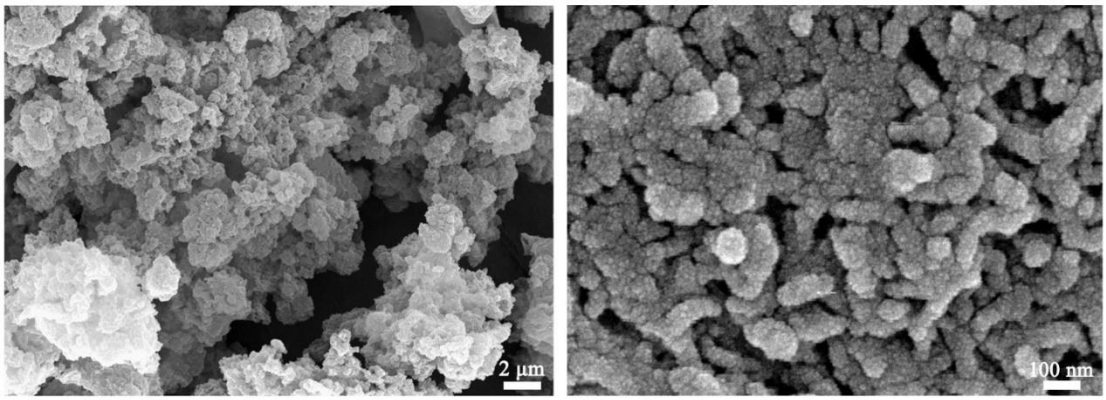

Fig. S2 SEM images of n-CTP.

III. Iodine adsorption of n-CTP

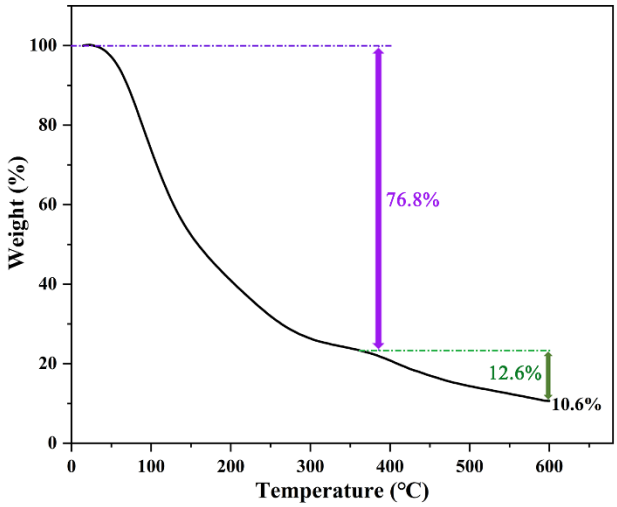

Fig.S3 TGA curve of the saturated n-CTP@I_2 (in N_2 atmosphere).

Table. S1 Gravimetric iodine uptake of n-CTP at different time at 25 °C.

Time (h)	Iodine uptake (g g^{-1})
1	0.2375
3	0.4250
6	0.825
24	1.9125
48	2.5625
72	2.7125

Table. S2 The kinetic parameters for iodine adsorption by n-CTP.

$q_{e,exp}$ ($g\ g^{-1}$)	Pseudo-firet-order kinetic model			Pseudo-second-order kinetic model		
	k_1 (min^{-1})	$q_{e,cal}$ ($g\ g^{-1}$)	R^2	k_2 ($g\ g^{-1}\ min^{-1}$)	$q_{e,cal}$ ($g\ g^{-1}$)	R^2
4.19	0.0128	3.998	0.981	0.00541	4.325	0.999

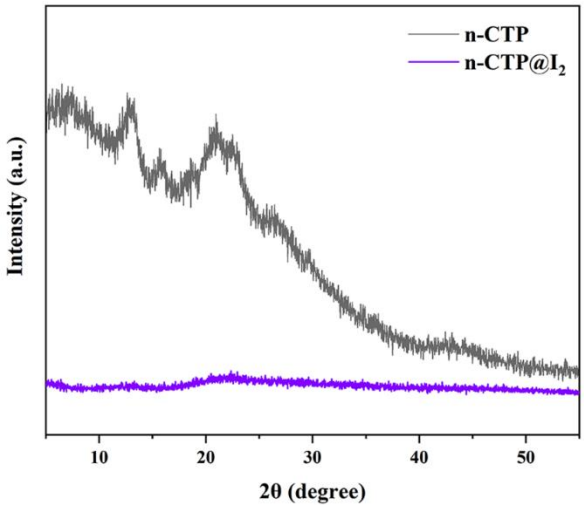

Fig. S4 PXRD patterns of n-CTP before and after iodine uptake.

Table. S3 Pore performance of reported adsorbents.

Porous adsorbent	BET surface area (m^2 g^{-1})	Pore size (Å)	Pore volume (cm^3 g^{-1})	Iodine uptake (g g^{-1})	R_{80} (g g^{-1} h^{-1})	Ref.
n-CTP	**207.13**	**34-100**	**0.586**	**4.19**	**1.34**	**This work**
TPT-BD COF	109	34.3	0.30	5.43	0.75	[3]
LNU-1	26	-	-	2.49	0.66	[4]
THPS-C	3125	-	1.60	3.40	0.54	[5]
TDTPAP	695.2	12.2	0.49	4.19	0.26	[6]
SIOC-COF-7	618	11.8	0.41	4.81	0.26	[2]
NiP-CMP	2630	7.0-12.5	2.288	2.02	0.25	[7]
AzoPPN	400	5.8-12.7	0.68	2.90	0.23	[8]
TTPDP	187.5	18.8	0.10	3.49	0.21	[6]
TTA-TTB	1733	22	1.01	4.95	0.10	[9]
TPB-DMTP	1927	33	1.28	6.26	0.17	[9]
SCMP-II	119.76	20	-	3.45	0.07	[10]

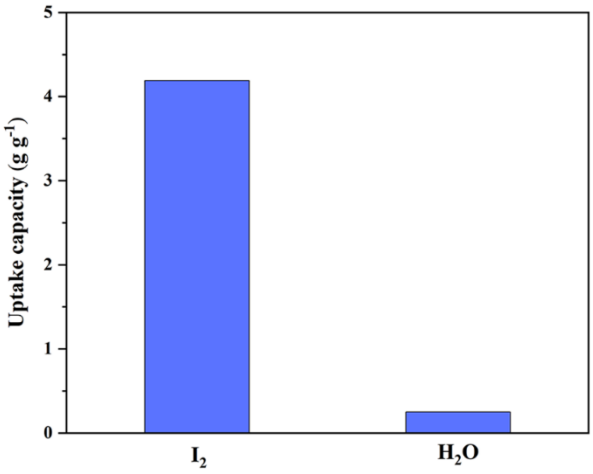

Fig. S5 The adsorption selectivity of n-CTP for I_2, water.

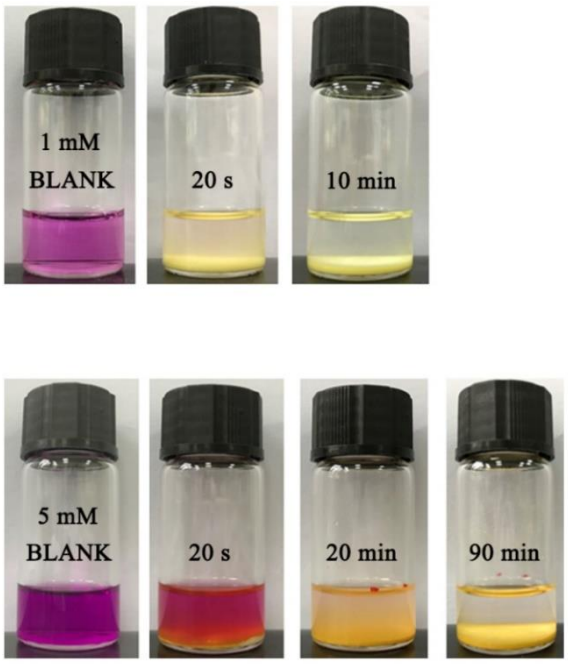

Figure. S6 Photographs show the color change of I_2 enrichment progress when 20 mg of n-CTP was immersed in a cyclohexane solution of iodine (1 mmol L^{-1}, 5 mmol L^{-1}, 3 mL).

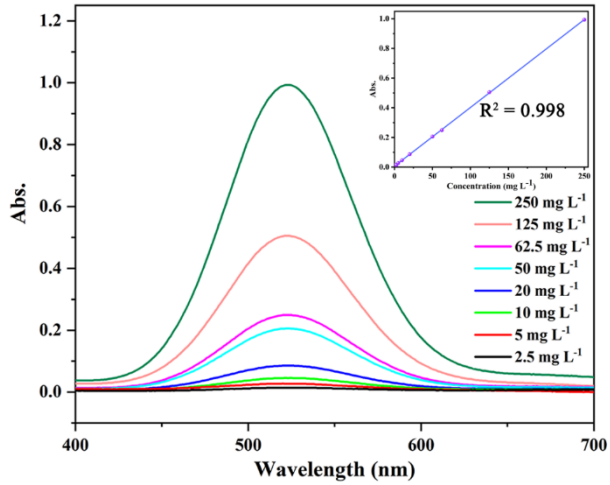

Figure. S7 Calibration plot of standard iodine by UV/vis spectra in cyclohexane solution. Inset: the fitting of Abs value vs concentration of I_2 with the relatively good linearity satisfies Lambert-Beer Law.

Table. S4 The kinetic parameters for iodine adsorption on n-CTP in cyclohexane solutions.

$q_{e,\,exp}$ (mg g^{-1})	Pseudo-firet-order kinetic model			Pseudo-second-order kinetic model		
	k_1 (min^{-1})	$q_{e,\,cal}$ (mg g^{-1})	R^2	k_2 (g mg^{-1} min^{-1})	$q_{e,\,cal}$ (mg g^{-1})	R^2
425.5	0.604	240.6	0.946	0.0076	434.8	0.999

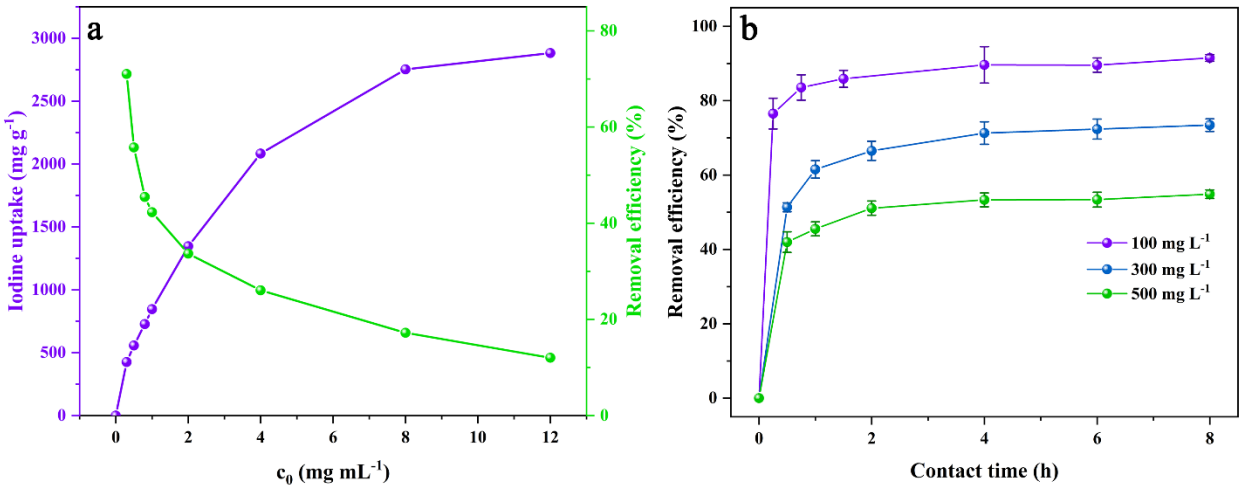

Fig. S8 Effect of initial concentration on the uptake capacity and removal efficiency (a) and effect of contact time on the removal efficiency (b) of iodine onto n-CTP in cyclohexane solutions (m/V = 0.5 g L^{-1}, t = 12 h). Error bars represent S.D. (standard deviation), n = 3 independent experiments.

As illustrated in Fig.S8, as the initial iodine solution concentration increases, the removal efficiency of n-CTP decreases and the adsorption capacity increases.

Table. S5 The parameters for Langmuir and Freundlich isotherm models of iodine adsorption by n-CTP.

$q_{e,exp}$ (mg g^{-1})	Langmuir isotherm model			Freundlich isotherm model		
	K_L (L mg^{-1})	q_m (mg g^{-1})	R^2	K_F (mg g^{-1})	1/n	R^2
2880	0.0035	1667	0.833	55.74	0.437	0.986

Refernce

1. T. Geng, W. Zhang, Z. Zhu and X. Kai, *Microporous Mesoporous Mater.*, 2019, **273**, 163-170.
2. Z. Yin, S. Xu, T. Zhan, Q. Qi, Z. Wu and X. Zhao, *Chem. Commun.*, 2017, **53**, 7266-7269.
3. X. Guo, Y. Tian, M. Zhang, Y. Li, R. Wen, X. Li, X. Li, Y. Xue, L. Ma, C. Xia and S. Li, *Chem. Mater.*, 2018, **30**, 2299-2308.
4. L. Xia, D. Yang, H. Zhang, Q. Zhang, N. Bu, P. Song, Z. Yan and Y. Yuan, *RSC Adv.*, 2019, **9**, 20852-20856.
5. Q. Zhang, T. Zhai, Z. Wang, G. Cheng, H. Ma, Q. Zhang, Y. Zhao, B. Tan and C. Zhang, *Adv. Mater. Interfaces*, 2019, **6**, 1900249.
6. T. Geng, C. Zhang, C. Hu, M. Liu, Y. Fei and H. Xia, *New J. Chem.*, 2020, **44**, 2312-2320.
7. S. A, Y. Zhang, Z. Li, H. Xia, M. Xue, X. Liu and Y. Mu, *Chem. Commun.*, 2014, **50**, 8495-8498.
8. H. Li, X. Ding and B. Han, *Chem. Eur. J.*, 2016, **22**, 11863-11868.
9. P. Wang, Q. Xu, Z. Li, W. Jiang, Q. Jiang and D. Jiang, *Adv. Mater.*, 2018, **30**, 1801991.
10. F. Ren, Z. Zhu, X. Qian, W. Liang, P. Mu, H. Sun, J. Liu and A. Li, *Chem. Commun.*, 2016, **52**, 9797-9800.